HHS Public Access

Author manuscript

Mol Imaging Biol. Author manuscript; available in PMC 2017 August 01.

Published in final edited form as:

Mol Imaging Biol. 2016 August ; 18(4): 483–489. doi:10.1007/s11307-015-0914-9.

Tc-99m Radiolabeled Peptide p5+14 is an Effective Probe for SPECT Imaging of Systemic Amyloidosis

Stephen J. Kennel[1,2,3], **Alan Stuckey**[2], **Helen P. McWilliams-Koeppen**[1], **Tina Richey**[1], and **Jonathan S. Wall**[1,2]

[1]Department of Medicine, University of Tennessee, Graduate School of Medicine, Knoxville, TN, USA

[2]Department of Radiology, University of Tennessee, Graduate School of Medicine, Knoxville, TN, USA

[3]University of Tennessee Medical Center, 1924 Alcoa Highway, Knoxville, TN, 37920, USA

Abstract

Purpose—Systemic peripheral amyloidosis is a rare disease in which misfolded proteins deposit in various organs. We have previously developed I-124 labeled peptide p5+14 as a tracer for positron emission tomography imaging of amyloid in patients. In this report, we now document the labeling efficiency, bioactivity, and stability of Tc-99m labeled p5+14 for single-photon emission computed tomography (SPECT) imaging of amyloidosis, validated in a mouse model of systemic amyloidosis.

Procedures—Radiochemical yield, purity, and biological activity of [^{99m}Tc]p5+14 were documented by instant thin-layer chromatography (ITLC), SDS-PAGE and a quantitative amyloid fibril pulldown assay. The efficacy and stability were documented in serum amyloid protein A (AA) amyloid-bearing or wild-type (WT) control mice imaged with SPECT/X-ray computed tomography (CT) at two time points. The uptake and retention of [^{99m}Tc]p5+14 in hepatosplenic amyloid was evaluated using region of interest (ROI) and tissue counting measurements.

Results—Tc-99m p5+14 was produced with a radiochemical yield of 75 % with greater than 90 % purity and biological activity comparable to that of radioiodinated peptide. AA amyloid was visualized by SPECT/CT imaging with specific uptake seen in amyloid-laden organs at levels ~5 folds higher than in healthy mice. ROI analyses of decay-corrected SPECT/CT images showed <20 % loss of radiolabel from the 1 to 4 h imaging time points. Biodistribution data confirmed the

Correspondence to: Stephen Kennel; skennel@utmck.edu.

Compliance with Ethical Standards

Ethical Statement

All animal studies were performed in accordance with protocols approved by the University of Tennessee Institutional Animal Care and Use Committee and in accordance with the guidelines provided by Office of Laboratory Animal Welfare (OLAW) and the Guide for the Care and Use of Laboratory Animals. The University of Tennessee Graduate School of Medicine is a AAALAC-I-accredited institution.

Conflict of Interest

JSW and SJK are inventors on a US patent (# 8.808 666) that describes the use of peptide p5 as an imaging agent for amyloidosis. JSW, SJK, TR, and AS are owners of Solex LLC, which sub-licensed rights to intellectual property from the University of Tennessee.

specificity of the probe accumulation by amyloid-laden organs as compared to non-diseased tissues.

Conclusion—[^{99m}Tc]p5+14 is a specific and stable radiotracer for systemic amyloid in mice and may provide a convenient and inexpensive alternative to imaging of peripheral amyloidosis in patients.

Keywords

Peptide p5+14; Technetium-99m; AA amyloid; Molecular imaging radiotracer

Introduction

Amyloidosis is a disease in which extracellular protein fibrils are deposited in various organs leading to morbidity and high mortality rates [1–3]. The most common form of amyloid disease involves the deposition of Aβ peptides, as fibrils, in the brains of patients with Alzheimer's disease [4, 5]. In addition, amyloid fibrils composed of many structurally and functionally diverse circulating proteins can deposit in peripheral organs [6]. These forms of systemic amyloidoses, while much less common than Alzheimer's disease, affect a significant population and, due to their rarity and the heterogeneity of clinical presentation, are likely underdiagnosed [7]. The amyloid load and anatomic distribution can best be evaluated by molecular imaging [8]. Serum amyloid P (SAP) component, labeled with I-123, has proven to be a useful radiotracer for planar scintigraphy and single-photon emission computed tomography (SPECT) imaging of peripheral amyloid in the UK and Europe [8, 9]. This imaging agent provides valuable information on the whole body distribution of visceral amyloid; however, it does not image cardiac amyloid effectively and it is not approved for use in the USA. Thus, there are currently no approved clinical radiotracers for the detection of systemic amyloid in the USA, and the radiotracers developed for cerebral Aβ amyloid imaging do not work well for the detection of systemic amyloid disease in multiple anatomic sites [10, 11].

In an effort to develop imaging technologies for systemic disease, we have identified several polybasic peptides that bind a diverse cadre of amyloid fibrils and, when radio-iodinated, can be used to specifically detect amyloid in a mouse model of systemic inflammation-associated serum amyloid protein A (AA) amyloidosis by using small animal imaging [12, 13]. After evaluating a series of structurally related peptides for their ability to bind amyloid specifically, we have identified a lead candidate, designated peptide p5+14 [14]. This peptide has been studied thoroughly as an iodinated, amyloid-specific radiotracer with the intent of using I-124 labeled peptide as a positron emitting probe for positron emission tomography (PET) imaging of systemic amyloid in a human clinical trial. This translational effort has received support from the Science Moving toward Research Translation and Therapy (SMARTT) Program at the NHLBI.

Recently, we have worked to develop a Tc-99m labeled variant of peptide p5+14 that we anticipate may be more clinically accessible due to reduced imaging costs and the availability of gamma scintigraphy and single-photon emission computed tomography (SPECT) in the clinic. In our initial preclinical studies, the peptides that we evaluated were

synthesized with Cys-Gly-Gly-Tyr-amino acids at the N-terminal to allow direct Tc-99m labeling using commercial pertechnetate saline stocks with stannous chloride as the reducing agent, according to the methods of Tran et al. [15]. However, peptides containing free Cys amino acids can present some stability problems on storage leading to complications with FDA approval for clinical applications. We, therefore, synthesized a peptide p5+14 variant with a Gly-Gly-Gly-Tyr (GGGY)-N-terminal leader sequence and found that it could be equally effectively radiolabeled with Tc-99m using the same direct method. In the work presented herein, we document the efficiency, stability, and effectiveness of Tc-99m labeled GGGY-p5+14 (hereafter referred to as p5+14) as a radiotracer for systemic amyloid disease using, as a model system, systemic inflammation-associated AA amyloidosis in mice.

Methods

Peptides

All peptides, including peptide p5+14, [GGGYS KAQKA QAKQA KQAQK AQKAQ AKQAK QAQKA QKAQA KQAKQA] were purchased from Anaspec (Fremont, CA) and further purified by reverse-phase high-pressure liquid chromatography (HPLC), as described previously [14].

Radiolabeling

Incorporation of Tc-99m was achieved according to the method of Tran et al. [15] with modifications as described below. To 20 μl of 0.15 N NaOH in a 1.5-ml plastic micro-centrifuge tube was added in order: 20 μl of peptide in water (10–100 μg) and 10 μl of 100 μg/ml of stannous chloride dihydrate ($SnCl_2 \cdot 2H_2O$). The tin solution was freshly prepared by adding 10 μl of 1 N HCl to 1 mg of $SnCl_2$ in a 1.5-ml microfuge tube to give a uniform suspension of 100 mg/ml, which was diluted with 1 ml of pure water to yield a stock solution of 1 mg/ml. The stock was further diluted 1/10 in 0.01 N HCl to give the final 100 μg/ml solution. Tc-99m, as pertechnetate (1–10 mCi in 100–300 μl of saline; Cardinal Health, Knoxville, TN), was added immediately. After incubating for 15 min at RT, the radiolabeled peptides were purified by gel filtration using a 5-ml Sephadex G25 size-exclusion matrix (PD10 column—GE Healthcare, Biosciences AB) equilibrated with 0.1 % gelatin in sterile phosphate buffered saline (PBS). Fractions eluting at the void volume with the blue dextran marker were pooled and the recovered radioactivity used to calculate radiochemical yield.

Assessment of Radiochemical Purity

Radiolabeled peptide was characterized by instant thin-layer chromatography (ITLC) on silica gel 60 strips (Selecto Scientific, Suwanee, GA) with a mobile phase consisting of a 1:1 mixture of 1 M aqueous ammonium acetate (NH_4OAc):methanol. Using this solvent, the peptide remains at the origin (rf=0) and TcO_4^- moves with the solvent front rf 1.0 [16]. Developed strips were imaged with an ITLC reader (BioScan 1000) and the purity calculated using regions of interest drawn in the WINSCAN software (BioScan Inc, Washington DC). Radiolabeled peptides were also analyzed by using SDS-PAGE followed by phosphorimaging (Cyclone phosphor Imager, Packard, Downers Grove, IL).

Evaluation of Bioactivity

Bioactivity of peptide [^{99m}Tc]p5+14 was assessed by assaying binding with fibrils composed of synthetic human λ6 variable domain (rVλ6Wil; [17]). Briefly, radiolabeled peptide (~10 ng, ~100,000 cpm) was added to a suspension of amyloid fibrils (~25 μg in 200 μl of PBS). The sample was mixed end over end using an orbital rotator for 1 h at RT. The insoluble fibril fraction was isolated by centrifugation at 15,000×*g* for 5 min, and after a wash step using PBS, the bound radioactivity was measured by using a Packard Cobra gamma scintillation counter (PerkinElmer, Shelton, CT). The percentage of [^{99m}Tc]p5+14 bound to the fibril pellet was determined as follows:

$$\%\,\mathrm{Bound} = \mathrm{Pellet\ cpm} / (\mathrm{Pellet\ cpm} + \mathrm{Supernatant\ cpm}) \times 100$$

SPECT/CT Imaging

Systemic AA amyloidosis was induced in H2-L^{d}-huIL-6 Tg Balb/c transgenic mice (H2/IL-6 mice) that constitutively express the human interleukin-6 transgene [18, 19] by iv injection of 10 μg of purified, splenic AA amyloid (amyloid-enhancing factor; AEF) suspended in 100 μl of sterile PBS. Mice were tested 4 to 6 weeks post AEF injection when large amounts of amyloid were present, but animals were not yet moribund. Control mice were non-transgenic, healthy mice of the same strain and approximate age hereafter referred to as wild-type (WT) mice.

Radiolabeled [^{99m}Tc]p5+14 (~5 μg, 500 μCi) was injected iv in the lateral tail vein in cohorts of 3 mice—AA amyloid mice or WT healthy controls. After a 1-h uptake period, SPECT/X-ray computed tomography (CT) images were acquired under anesthesia (2 % isoflurane in oxygen) using a small animal imaging chamber (M2M, Cleveland, OH). At 4 h post-injection, the mice were euthanized by inhalation of an overdose of air saturated with isoflurane and SPECT/CT imaging performed again. Image data were collected using an Inveon trimodality SPECT/PET/CT platform (Siemens Preclinical, Knoxville, TN; [20]). Briefly, SPECT images were generated by acquiring 90 16-s projections over a total of 1.5 detector revolutions. A 1.0-mm-diameter five-pinhole (mouse whole body) collimator was used at 30 mm from the center of the field of view. The data were reconstructed using a maximum a priori (MAP) algorithm with 3D ordered subset expectation maximization (OSEM; 16 iterations, 6 subsets, β=1). Images were reconstructed onto a matrix with *x, y, z* dimension of 88×88×312 and 0.5-mm isotropic voxels. Attenuation correction was applied to data using the CT image data. Scatter correction was applied to the SPECT data using a triple-energy window (TEW) method [21]. The 4 h SPECT image data were decay-corrected to the 1 h imaging time point, using standard procedures, to allow quantitative comparison.

CT images were acquired using an X-ray voltage biased to 80 kVp with a 500-μA anode current. Two bed positions were acquired with 240 ms exposure and 361 projections collected covering 360° of continuous rotation. The data were reconstructed using an implementation of the Feldkamp filtered cone-beam algorithm [22] onto a 256×256×603 matrix with isotropic 211.4-μm voxels.

Biodistribution

Following the second SPECT/CT image acquisition, a necropsy was performed and samples from 11 tissues were taken for radioactivity biodistribution analyses. The tissue samples were placed in tared vials and the radioactivity measured using an automated Wizard 3 gamma counter (1480 Wallac Gamma Counter, PerkinElmer). Data were decay-corrected to the time of injection and expressed as % injected dose per gram of tissue (%ID/g).

Ethical Statement

All animal studies were performed in accordance with protocols approved by the University of Tennessee Institutional Animal Care and Use Committee and in accordance with the guidelines provided by Office of Laboratory Animal Welfare (OLAW) and the Guide for the Care and Use of Laboratory Animals. The University of Tennessee Graduate School of Medicine is a AAALAC-I-accredited institution.

Results

Reaction Conditions

The standard method of radiolabeling, as described in the “Methods” section, was adopted after a number of preliminary trials to optimize the concentrations of reagents and reaction times. Our data showed that, when labeling small quantities of peptide (*e.g.*, 10–100 μg), 1 μg of $SnCl_2$ and short reaction times of ~5–15 min were adequate. Data in Fig. 1 show ITLC evaluation for the reaction of [^{99m}Tc]per-technetate with peptide p5+14 or for reaction mixtures lacking peptide (mock labeling). In the reaction mixture containing p5+14, after 1 min incubation, most of the Tc-99m remained at the origin of the ITLC (Fig. 1a, arrowhead). By 15 min of incubation, nearly all of the Tc-99m was at the origin indicating completion of the reaction and no free radionuclide (Fig. 1b). In contrast, in the peptide-free reaction, after 1 min (Fig. 1c), ~10 % Tc-99m remained at the origin, consistent with the formation of TcO_2 colloid [16]. However, after the 15 min incubation, there was no evidence of colloid (Fig. 1d). Based on these data, the 15-min reaction time was adopted as standard.

Characterization of [^{99m}Tc]p5+14

The radiolabeled peptide product was purified by gel filtration, as described, and re-evaluated in ITLC. The product was deemed to be ~92 % pure by this evaluation (Fig. 1e) and, after 6 h at RT, was still at 76 % radiopurity (data not shown). Purified [^{99m}Tc]p5+14 was diluted into non-reducing SDS-PAGE loading buffer and then loaded onto the gel with or without boiling for 5 min. Phosphor-imager analysis of the gel revealed bands corresponding to the appropriate peptide mass (~3000 Da) and were shown to be >90 % pure using image analysis software (Fig. 1f). The radiochemical yield was 75±7.7 % (n=6). The reactivity of the radiolabeled product was evaluated in a pulldown assay using synthetic rVλ6Wil AL amyloid fibrils. In eight independent studies, the radiolabeled p5+14 yielded values of 58±14 % bound to fibrils.

SPECT/CT Imaging

Two SPECT/CT image data sets were collected for each AA-laden and WT mouse at 1 and 4 h post injection to assess the stability of the [^{99m}Tc]p5+14 when bound to visceral amyloid in the liver and spleen—major sites of disease in this animal model. Dramatic differences were observed in the SPECT images of [^{99m}Tc]p5+14 in AA mice at 1 and 4 h pi (Fig. 2a, b, respectively) as compared to WT mice (Fig. 2c, d). Mice with AA amyloid accumulated the radiotracer principally in the intestines (Int), liver (Liv), and spleen, consistent with the specific interaction of peptide with hepatosplenic and intestinal amyloid deposits. Histochemical evaluation of the visceral organs from the AA mice, harvested at necropsy, confirmed the presence of amyloid in these anatomic sites (data not shown). In contrast, in healthy mice, Tc-99m was observed in the intestines and bladder, consistent with hepatobiliary and renal clearance of the [^{99m}Tc]p5+14, respectively. Notably, the bladder (Bla) was readily visible in the WT mouse at 1 h post injection, indicating that a significant amount of Tc-99m remained associated with the peptide during clearance into the urinary bladder.

For image quantitative analysis, regions of interest (ROI) were drawn in the liver and spleen of 2D images (1 and 4 h pi SPECT data sets). As anticipated from the image data, the liver and spleen values (expressed as arbitrary SPECT units) were up to 10-fold higher in AA mice as compared to those from WT mice (Table 1). Furthermore, values for the 1 and 4 h decay-corrected scans showed little loss of Tc-99m from the liver or spleen in AA mice (83 % retention in the liver and 116 % retention in the spleen) indicating that ^{99m}Tc was not rapidly dissociated from the amyloid-bound [^{99m}Tc]p5+14 in the extracellular space. The large variability in ROI measurements for spleen likely reflects the fact that the spleen is small, and ROI data were contaminated by “spillover” in the image due to the proximity of the kidney and stomach which have high accumulation in the AA and WT mice, respectively.

Biodistribution

The uptake of [^{99m}Tc]p5+14 in each organ at 4 h pi was quantified by tissue biodistribution measurements and expressed as %ID/g (Fig. 2e). Considering both the imaging data and the biodistribution data in WT mice, it is clear that most of the excretion of unbound probe occurs through the kidney and bladder with possibly a small amount of elimination through the hepatobiliary system. The fact that kidneys of the WT mice retain a larger fraction of ^{99m}TC p5+14 as compared to AA mice is due to retention of the radiotracer in visceral amyloid deposits in the AA mice and also a decrease in renal function as a result of the amyloidosis. From evaluating the biodistribution data at 4 h post injection, it is clear that with the exception of kidneys, all organs that contain amyloid in the AA mice—liver, pancreas, spleen, stomach, intestines, and heart—retain more Tc-99m labeled peptide than those organs in the amyloid-free WT mice. Furthermore, these data are consistent with published values for biodistribution of this peptide radiolabeled with iodide isotopes [14].

Discussion

The need for an imaging agent for patients with systemic visceral amyloid disease has been documented elsewhere [8, 12, 14]. Although numerous imaging agents including [^{123}I]SAP [8, 9], [^{99m}Tc]aprotinin [23, 24], I-124 radio-labeled 11-1F4 antibody [25], Tc-99m labeled bone-seeking agents [26, 27], and radiofluorinated Aβ amyloid detection agents [10, 11] have been evaluated for use in peripheral amyloidosis patients, each has its limitations with respect to the ability for quantitative imaging of amyloid in patients with the diverse amyloid diseases. We have evaluated a series of polybasic peptides for their ability to bind these multiple forms of amyloid by using histochemistry on human amyloid-laden tissue sections and in a mouse model of severe systemic AA amyloidosis [12–14]. The most promising peptide for translation into the clinic, p5+14, has been effectively radioiodinated with I-125, I-123, and I-124 for SPECT and PET imaging of amyloid [14]. However, since most clinical nuclear medicine facilities are more familiar with Tc-99m chemistry and SPECT imaging protocols and because Tc-99m is considerably less expensive than radioiodide isotopes, we evaluated methods for Tc-99m labeling of the p5+14 peptide.

For our preliminary studies, we designed a variant of the p5+14 peptide with an N-terminal Cys to permit direct coupling of Tc-99m via a Cys-Gly-Gly motif [15]. However, removal of the N-terminal Cys was deemed important in the translation of the peptide into clinical trials, as this moiety may promote undesirable disulfide crosslinking of the peptides and consequent structural heterogeneity in the drug product. Therefore, we synthesized p5+14 with Gly as the N-terminal amino acid, and we found that $SnCl_2$ reduction of [^{99m}Tc]TcO_4^- efficiently generated [^{99m}Tc]p5+14 peptide even in the absence of the Cys residue. Furthermore, we demonstrated that the amount of $SnCl_2$ and the reaction times could be reduced approximately 10-fold and still achieve recoveries of radiolabeled p5+14 of ~75 %. In fact, we have successfully radiolabeled a variety of peptides with diverse amino acid compositions using Tc-99m by this facile method (data not shown).

The precise nature of the chemical interaction of the Tc-99m compounds in various ionic states with the peptide is very difficult to establish by standard chemical analyses due to the minute concentrations involved. There has been great interest in Tc-99m chemistry as it relates to conjugation with peptides and proteins as probes for SPECT imaging. One of the most comprehensive reviews of the several different methods is presented by Boerman [28]. The majority of the chemical methods involve the multidentate chelation of Tc-99m (V) ions, produced by Sn^{+2} reduction, to amino acid ligands and co-ligands or interaction with nitroimidazole rings (HYNIC). Numerous different labeling methods and specific applications have been published since the review by Boerman. Most, if not all, involve products of [^{99m}Tc]TcO_4^- reduced by the addition of Sn^{+2} (presumably Tc-99m (V) compounds) and bound to peptides through various chelating structures. Previously, bovine aprotinin (a 58 amino acid trypsin inhibitor) has been radiolabeled with Tc-99m using $SnCl_2$ reduction conditions similar to those used herein [29] and has been subsequently used to monitor renal function [30] and detect cardiac amyloid disease by using planar gamma scintigraphy [23, 24]. Although available in Europe, bovine aprotinin (Trasylol™, Bayer AG) is no longer available in the USA; however, the positive amyloid-imaging results augur well for our proposed trial using the amyloidophilic peptide p5+14. In addition, the current

state of the art in whole-body SPECT can provide enhanced image quality in a shorter time and is an excellent alternative to gamma scintigraphy.

The structure of [^{99m}Tc]aprotinin [29] and that of [^{99m}Tc]p5+14 have not been well characterized; although, given the heterogeneity in amino acid sequence between the two, radiolabeling may involve the peptide backbone as opposed to the amino acid side-chain moieties. This is further supported by the fact that we have successfully coupled Tc-99m to many peptides with different amino acid sequences, net charge (basic and acidic), and secondary structure (Kennel and Wall, unpublished data). Alternatively, it is possible that the N-terminal three glycine motif provides the chelation structure; although, most triglycine methods require tricine as a co-ligand which is absent from our radiolabeling procedure.

Given the enigmatic complexity of peptide radiolabeling with Tc-99m, we have not attempted an exhaustive investigation of the structure of the [^{99m}Tc]p5+14 peptide; rather, we have taken an applied approach by evaluating the radiochemical yield, purity, bioactivity, and stability of Tc-99m labeled p5+14 *in vivo*, using a standard procedure, in anticipation of using [^{99m}Tc]p5+14 in the clinical setting for imaging amyloid in patients. The [^{99m}Tc]p5+14 radiotracer can be prepared reproducibly and in high yields with reaction conditions easily adapted to clinical nuclear medicine facilities. Purified product has been shown to be ~90 % radiochemically pure and maintains high biologic activity in amyloid fibril-specific binding assays. The Tc-99m remains stably associated with the peptide even when boiled and in the presence of a peptide denaturing agent, SDS (Fig. 1f). When [^{99m}Tc]p5+14 was injected into AA amyloid-laden mice, it accumulated efficiently in amyloid-containing organs where it remained stably radiolabeled for at least 4 h post injection (Fig. 2 and Table 1). The accumulation and retention of radiolabeled p5+14 in amyloid *in vivo* recapitulates similar data obtained using radioiodinated p5+14 [14]. Thus, regardless of the chemical nature of the radiolabeling with Tc-99m, the electrostatic interactions which govern the binding of p5+14 with amyloid are not compromised. The [^{99m}Tc]p5+14 retains amyloid specificity and exhibits *in vivo* stability as evidenced by quality assurance assays, serial SPECT/CT scanning, and biodistribution data and may, therefore, be suitable for clinical imaging purposes.

Effective probes for molecular imaging must be rapidly cleared if they are not stably bound to the target. Radio-iodinated proteins and peptides, used for amyloid imaging, have the advantage that unbound radiotracer is rapidly dehalogenated in the liver or kidneys. The resulting free radioiodide then re-enters the circulation and is rapidly sequestered by the stomach and thyroid allowing efficient imaging of other organs. In contrast, ^{99m}Tc remains primarily bound to the peptide even without the use of chelating agents as we have shown in this study. Consequently, radioactivity is slower to clear from the sites of catabolism, notably the kidneys. This property of the Tc-99m radiolabeled p5+14 peptide may hinder detection of amyloid in the kidney; however, this remains to be evaluated in clinical trials. The fact that [^{99m}Tc]p5+14 is easy to prepare, inexpensive, can be made readily available to a large number of clinical sites and may provide imaging of cardiac amyloid are potential advantages for use of this radiotracer as a routine clinical tool for detection and monitoring amyloid deposits in patients.

Conclusion

Tc-99m labeled p5+14 peptide is easily prepared, and if used for planar gamma scintigraphic or SPECT imaging, it affords a relatively inexpensive and reproducible alternative to radioiodinated peptide for the non-invasive detection of systemic visceral amyloidosis disease *in vivo*.

Acknowledgments

This work was supported by PHS grant R01DK079984 from The National Institute of Diabetes and Digestive and Kidney Diseases (NIDDK), as well as funds from the Molecular Imaging and Translational Research Program, and Department of Medicine at UTMCK. We thank Dr. Emily Martin for help in proofreading and annotating this article.

Abbreviations

AA	Serum amyloid protein A
SPECT/CT	Single-photon emission computed/X-ray computed tomography
ARG	Microautoradiography

References

1. Merlini G, Wechalekar AD, Palladini G. Systemic light chain amyloidosis: an update for treating physicians. Blood. 2013; 121:5124–5130. [PubMed: 23670179]
2. Obici L, Merlini G. AA amyloidosis: basic knowledge, unmet needs and future treatments. Swiss Med Wkly. 2012; 142:w13580. [PubMed: 22653707]
3. Pepys MB. Amyloidosis. Ann Rev Med. 2006; 57:223–241. [PubMed: 16409147]
4. Kumar A, Singh A, Ekavali. A review on Alzheimer's disease pathophysiology and its management: an update. Pharmacol Rep. 2015; 67:195–203. [PubMed: 25712639]
5. Masters CL, Selkoe DJ. Biochemistry of amyloid beta-protein and amyloid deposits in Alzheimer disease. Cold Spring Harb Perspect Med. 2012; 2:a006262. [PubMed: 22675658]
6. Blancas-Mejia LM, Ramirez-Alvarado M. Systemic amyloidoses. Annu Rev Biochem. 2013; 82:745–774. [PubMed: 23451869]
7. Pinney JH, Smith CJ, Taube JB, et al. Systemic amyloidosis in England: an epidemiological study. Br J Haematol. 2013; 161:525–532. [PubMed: 23480608]
8. Hawkins PN. Diagnosis and monitoring of amyloidosis. Baillieres Clin Rheumatol. 1994; 8:635–659. [PubMed: 7954867]
9. Hazenberg BP, van Rijswijk MH, Piers DA, et al. Diagnostic performance of 123I-labeled serum amyloid P component scintigraphy in patients with amyloidosis. Am J Med. 2006; 119(355):e315–324.
10. Dorbala S, Vangala D, Semer J, et al. Imaging cardiac amyloidosis: a pilot study using (1)(8)F-florbetapir positron emission tomography. Eur J Nucl Med Mol Imaging. 2014; 41:1652–1662. [PubMed: 24841414]
11. Osborne D, Acuff S, Stuckey A, Wall J. A routine PET/CT protocol with simple calculations for assessing cardiac amyloid using 18F-Florbetapir. Frontiers in Cardiovascular Medicine. 2015:2. [PubMed: 26664874]
12. Wall JS, Richey T, Stuckey A, et al. In vivo molecular imaging of peripheral amyloidosis using heparin-binding peptides. Proc Natl Acad Sci U S A. 2011; 108:E586–594. [PubMed: 21807994]
13. Wall JS, Williams A, Richey T, et al. A binding-site barrier affects imaging efficiency of high affinity amyloid-reactive peptide radiotracers in vivo. PLoS ONE. 2013; 8:e66181. [PubMed: 23750281]

14. Wall JS, Martin EB, Richey T, et al. Preclinical validation of the heparin-reactive peptide p5+14 as a molecular imaging agent for visceral amyloidosis. Molecules. 2015; 20:7657–7682. [PubMed: 25923515]
15. Tran T, Engfeldt T, Orlova A, et al. In vivo evaluation of cysteine-based chelators for attachment of 99mTc to tumor-targeting Affibody molecules. Bioconjug Chem. 2007; 18:549–558. [PubMed: 17330952]
16. Li F, Cheng T, Dong Q, et al. Evaluation of (99m)Tc-HYNIC-TMTP1 as a tumor-homing imaging agent targeting metastasis with SPECT. Nucl Med Biol. 2015; 42:256–262. [PubMed: 25516099]
17. Wall J, Schell M, Murphy C, et al. Thermodynamic instability of human lambda 6 light chains: correlation with fibrillogenicity. Biochem. 1999; 38:14101–14108. [PubMed: 10529258]
18. Solomon A, Weiss DT, Schell M, et al. Transgenic mouse model of AA amyloidosis. Am J Pathol. 1999; 154:1267–1272. [PubMed: 10233864]
19. Wall JS, Richey T, Allen A, et al. Quantitative tomography of early-onset spontaneous AA amyloidosis in interleukin 6 transgenic mice. Comp Med. 2008; 58:542–550. [PubMed: 19149411]
20. Magota K, Kubo N, Kuge Y, et al. Performance characterization of the Inveon preclinical small-animal PET/SPECT/CT system for multimodality imaging. Eur J Nucl Med Mol Imaging. 2011; 38:742–752. [PubMed: 21153410]
21. Ogawa K. Simulation study of triple-energy-window scatter correction in combined Tl-201, Tc-99m SPECT. Ann Nucl Med. 1994; 8:277–281. [PubMed: 7702973]
22. Feldkamp LA, Davis LC, Kress JW. Practical cone-beam algorithm. J Optical Soc Am A. 1984; 1:612–619.
23. Aprile C, Marinone G, Saponaro R, et al. Cardiac and pleuropulmonary AL amyloid imaging with technetium-99m labelled aprotinin. Eur J Nucl Med. 1995; 22:1393–1401. [PubMed: 8586084]
24. Schaadt BK, Hendel HW, Gimsing P, et al. 99mTc-aprotinin scintigraphy in amyloidosis. J Nucl Med. 2003; 44:177–183. [PubMed: 12571206]
25. Wall JS, Kennel SJ, Stuckey AC, et al. Radioimmunodetection of amyloid deposits in patients with AL amyloidosis. Blood. 2010; 116:2241–2244. [PubMed: 20522711]
26. Glaudemans AW, van Rheenen RW, van den Berg MP, et al. Bone scintigraphy with (99m)technetium-hydroxymethylene diphosphonate allows early diagnosis of cardiac involvement in patients with transthyretin-derived systemic amyloidosis. Amyloid. 2014; 21:35–44. [PubMed: 24455993]
27. Perugini E, Guidalotti PL, Salvi F, et al. Noninvasive etiologic diagnosis of cardiac amyloidosis using 99mTc-3,3-diphosphono-1,2-propanodicarboxylic acid scintigraphy. J Am College Cardiol. 2005; 46:1076–1084.
28. Boerman, OC. Radiochemistry of Technetium-99m. www.nkrv.nl/wp-content/uploads/2010/04/Tc99m_Boerman.pdf
29. Bianchi C, Donadio C, Tramonti G, et al. 99mTc-aprotinin: a new tracer for kidney morphology and function. Eur J Nucl Med. 1984; 9:257–260. [PubMed: 6204873]
30. Aprile C, Saponaro R, Villa G, et al. Assessment of split renal function with 99mTc-aprotinin. Eur J Nucl Med. 1986; 12:37–40. [PubMed: 2426112]

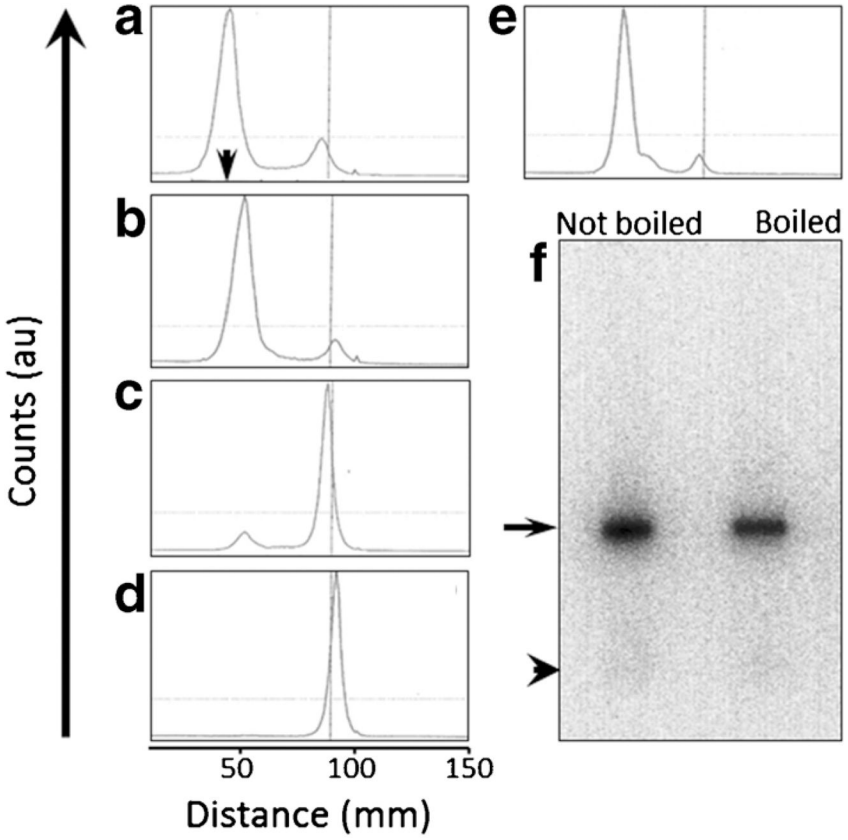

Fig. 1.

Documentation of purity of [^{99m}Tc]p5+14. Standard reaction conditions were used either with or without (mock) added peptide to test for the presence of Tc colloids. ITLC profiles (origin marked with an *arrow*) of the reaction mixture at **a** 1 and **b** 15 min after addition of TcO_4^-. Corresponding profiles for the mock reaction mixture are shown in **c** and **d**, respectively. **e** ITLC and **f** SDS-PAGE profiles of the purified final product demonstrate >90 % radiochemical purity. The *left lane* of the SDS-PAGE profile is for the sample in non-reducing loading buffer, but not boiled. The *right lane* is the same loading buffer, but boiled for 5 min before loading (*arrow* designates peptide mobility; *arrowhead* designates free Tc mobility).

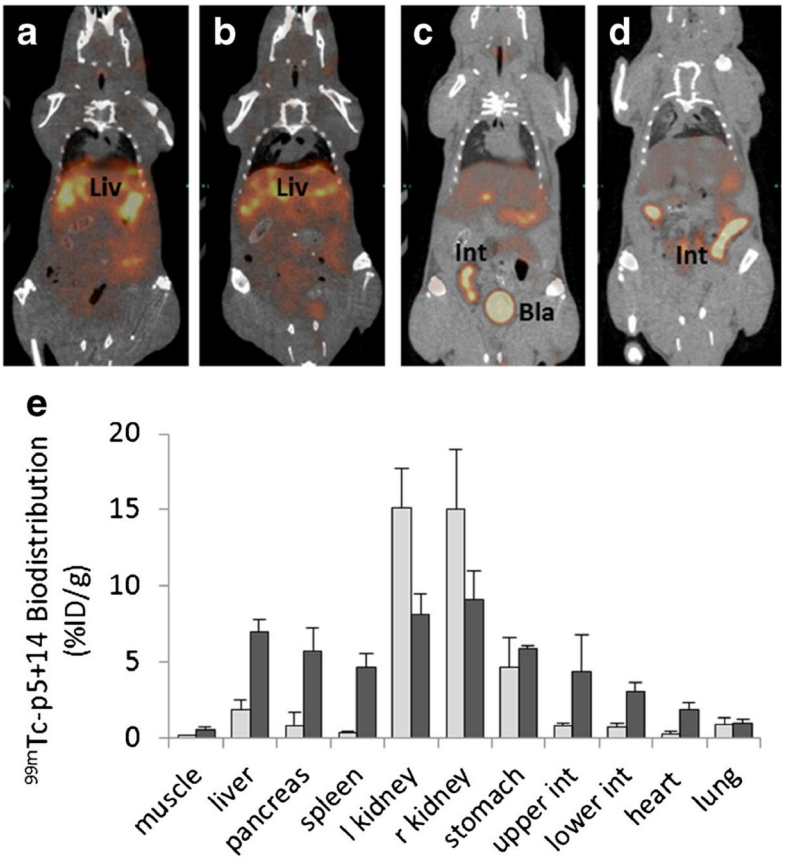

Fig. 2.

Decay-corrected SPECT/CT images of mice injected with ~5 μg, 500 μCi of [^{99m}Tc]p5+14 iv. Ventral views of an AA mouse at **a** 1 h pi and the same mouse postmortem at **b** 4 h pi. Corresponding images for a WT mouse at **c** 1 and **d** 4 h. *Int*—intestine, *Liv*—liver, *Bla*—bladder. **e** Biodistribution [mean %ID/g and standard deviation (n=3)] of [^{99m}Tc]p5+14, 4 h pi in AA mice (*dark bars*) or WT mice (*light bars*).

Mol Imaging Biol. Author manuscript; available in PMC 2017 August 01.

Table 1

Distribution of [^{99m}Tc]p5+14 in AA mice obtained from ROI analysis of decay-corrected SPECT images

Mouse	AA/WT	Organ	Activity at 1 h (mean au±SD[a])	Activity at 4 h (mean au±SD)	% Retention
1	AA	Liver	1725±128	1417±81	82
		Spleen	595±91	528±92	89
2	AA	Liver	1350±74	1015±108	75
		Spleen	514±59	577±82	112
3	AA	Liver	889±78	873±121	98
		Spleen	721±63	1019±156	141
4	WT	Liver	350±57	251±46	72
		Spleen	29±20	33±41	113
5	WT	Liver	398±53	301±62	76
		Spleen	45±22	21±15	47
6	WT	Liver	334±65	149±48	69
		Spleen	15±13	14±6	93

[a]Mean arbitrary units (au)±standard deviation (SD)